OPEN ACCESS
Journal of Innovative Optical Health Sciences
(2023) 2342001 (9 pages)

DOI: 10.1142/S1793545823420014

World Scientific
www.worldscientific.com

Effect of Sodium Nitroprusside on the microrheological properties of red blood cells in different media

Petr Ermolinskiy[*,§], Matvey Maksimov[*,¶], Andrei Lugovtsov[*,‖], Alexey Muravyov[†,**], Irina Tikhomirova[‡,††] and Alexander Priezzhev[*,‡‡]

[*]*Faculty of Physics, M.V. Lomonosov Moscow State University*
Moscow 119991, Russia

[†]*Faculty of Physical Education*
K.D. Ushinsky Yaroslavl State Pedagogical University
Yaroslavl 150000, Russia

[‡]*Faculty of Natural Sciences*
K.D. Ushinsky Yaroslavl State Pedagogical University
Yaroslavl 150000, Russia
[§]*ermolinskiy.pb15@physics.msu.ru*
[¶]*madoway@yandex.ru*
[‖]*anlug1@gmail.com*
[**]*alexei.47@mail.ru*
[††]*tikhom-irina@yandex.ru*
[‡‡]*avp2@mail.ru*

Received 28 July 2023
Revised 10 October 2023
Accepted 22 October 2023
Published 11 November 2023

Red blood cell (RBC) aggregation as well as their deformation significantly affects blood microrheology. These processes depend on various factors, one of which is concentration of the nitric oxide, one of the main signaling molecule in the bloodstream. The purpose of this study was to investigate the effect of nitric oxide on the microrheological properties of red blood cells (RBCs) in RBC samples of various media after the addition of nitric oxide donor sodium nitroprusside *in vitro*. Microrheological properties were measured using laser aggregometer and ektacytometer based on diffuse light scattering and diffraction of laser light on a suspension of RBCs, respectively. The study found that heparin-stabilized blood showed increased RBC aggregation and deformation with sodium nitroprusside concentrations of 100, and 200 μM, while EDTA-stabilized blood showed slightly decreased aggregation and unchanged deformation. With washed RBCs in dextran solution, the addition of sodium nitroprusside (in the concentrations of 100, and 200 μM) resulted in decreased aggregation and increased deformation. These findings aid in our understanding of nitric oxide's effect on RBC microrheological properties.

Keywords: Sodium nitroprusside; nitric oxide; red blood cells; RBC aggregation; diffuse light scattering; laser diffractometer.

1. Introduction

Blood consists of blood plasma, and blood cells, among which red blood cells (RBCs) predominate. RBC is a nucleus free and highly deformable cell. RBC has a shape of biconcave disc about 8 μm in diameter in the nonpathological state.[1] The primary function of RBCs is the transport of oxygen from the lungs to the tissues, and the transport of carbon dioxide and metabolic products in the opposite direction.[2] But there are other crucial functions in which RBCs play an important role such as blood clotting,[3] immune response,[4] and blood microrheology.[5]

Blood microrheology is mainly conditioned by RBC reversible aggregation, and deformation. These processes depend on a variety of endogenous, and exogenous factors, respectively, cellular, and media factors.[5–7] Under *in vivo* conditions, RBC aggregation, and deformation are regulated by various signaling mechanisms, including those involving signaling molecules, i.e., gasotransmitters.[8,9] In the bloodstream, one of the most important signaling molecules is nitric monoxide (NO). It is an unstable radical with a lifetime of about 100 ms and *in vivo* it is mostly secreted by the endothelial NO synthase.[10]

Regarding NO secretion, there are two groups of substances: compounds that release NO spontaneously (e.g., sodium nitroprusside) and those that require enzymatic metabolism to generate NO (e.g., L-Arginine).[11] As far as there is nitric oxide synthase in RBC, both groups of NO donors can affect RBC properties.[12]

The effect of NO donors, i.e., sodium nitroprusside (SNP), and L-Arginine, on the microrheological properties of RBCs has been investigated *in vitro* in a number of studies.[9,13–16] In these studies, it was shown that the deformability of RBC increases, and RBC aggregation diminishes under the influence of NO donors. It is a fair point to mention that RBC aggregation and RBC deformation was estimated in dextran solutions or highly diluted solutions.

In the literature, there is some evidence that the mechanisms of RBC aggregation as well as RBC deformation in blood plasma differ from the dextran solutions.[5,17] Mainly, it is assumed that RBC aggregation in blood plasma is more complex than in solution of artificial macromolecules, e.g., dextrans.[18] For *in vitro* studies of RBC aggregation, it is necessary to establish which anticoagulant is preferred and how it affects the measured parameters.

The aim of this study was to investigate the effect of nitric oxide on the microrheological properties of RBCs in RBC samples, i.e., whole blood stabilized with different anticoagulants (EDTA K3 or lithium heparin) or washed RBC resuspended in dextran solution (130 kDa), after the addition of nitric oxide donor SNP at different concentrations.

2. Materials and Methods

2.1. *Blood preparation*

The blood for all measurements was drawn from the cubital vein of 3 healthy male donors (22–25 years) on an empty stomach. All volunteers gave informed consent in accordance with the Declaration of Helsinki and the study was approved by the Ethics Committee of Medical Research and Educational Center of M.V. Lomonosov Moscow State University (protocol No. 11/22 05.12.2022). Tubes for blood samples contained EDTA K3 (1.2 mg in 1 mL of blood) or lithium heparin (12–30 IU in 1 mL of blood) anticoagulants. All experiments were performed within 6–7 h after blood sampling. The aggregation, and deformation properties of RBC do not undergo significant changes during this time.[19] The measurements in whole blood and in dextran solutions were conducted separately in different days (each donor gave blood twice for this study) to maintain the blood storage period.

SNP (Sigma-Aldrich; CAS Number:13755-38-9) was suspended in distilled water to the concentrations in the range 5–100 mM. The SNP solution was added to the RBC samples in ratio 1:100 (1 part of SNP solution, and 100 parts of blood) in order to obtain the final concentrations 0, 50, 100, 200, and 1000 μM. The control sample consists of 1 part of distilled water, and 100 parts of the blood sample.

2.1.1. *Whole blood samples preparation*

SNP was added to the whole blood stabilized by EDTA K3 or lithium heparin to obtain the following SNP concentrations: 0, 50, 100, 200, and 1000 μM. The incubation of whole blood with SNP was conducted for 30 min at 37°C before the measurements.

2.1.2. *Dextran RBC samples preparation*

To obtain washed RBC in dextran solution (130 kDa), the following steps were performed:

(1) Whole blood in a volume of 1.5 mL was poured into 2 mL tubes, and centrifuged for 10 min at 180 g under room temperature (22°C). The plasma layer with platelets was then removed by pipetting.
(2) 1 mL of PBS was added to the RBC volume, then the tube was stirred well to make suspension homogeneous. Then RBCs were washed in PBS for 3 min at 1000 g under room temperature (22°C).
(3) A mixture of Ringer's solution, and Voluven's solution (6% hydroxyethyl starch 130/0.4 in 0.9% sodium chloride) in the ratio 6:4 was prepared. The final concentration of dextran (hydroxyethyl starch) was 24 mg/mL, and the theoretical pH of the prepared solution was in the range 6.5–6.7 pH. Washed RBCs were added to the prepared solution until the hematocrit reached 40% just before the next step.
(4) SNP solution was added to the freshly prepared sample to obtain the following concentrations: 0, 50, 100, 200, and 1000 μM. The incubation of blood sample with SNP was conducted for 30 min at 37°C before measurements.

2.2. *RBC aggregation and deformation measurements*

Measurements of aggregation, and deformation parameters of RBC were assessed by diffuse light scattering[20] and laser ektacytometry techniques implemented in the RheoScan-AnD300 device (RheoMedTekh, Republic of Korea).[21,22]

2.2.1. *Diffuse light scattering technique*

RBC aggregation was quantified by the diffuse light scattering technique and several parameters were measured using two types of disposable test chips: RSD-K01 chip — micro-channel type allowing to measure the hydrodynamic strength of RBC aggregates, and RSA-C01 chip — allowing to measure parameters of the spontaneous RBC aggregation.[23] This method is based on the fact that RBCs and their aggregates scatter light differently.[24] Therefore, by measuring the intensity of light scattered from blood sample during spontaneous aggregation, the kinetic of RBC aggregation is measured.

The typical kinetic of the measured intensity of light scattered forward for RSA-C01 chip is presented in Fig. 1. At the beginning of the measurement, the RBCs were in a state of maximum aggregation, so the intensity of the scattered light was also maximum. Then, the magnetic stirrer breaks the aggregates, stops (point 0 on the time scale), and the process of spontaneous aggregation of RBCs begins. Aggregation index (AI) can be calculated, which characterizes the RBC spontaneous aggregation in the first 10 s of the process.

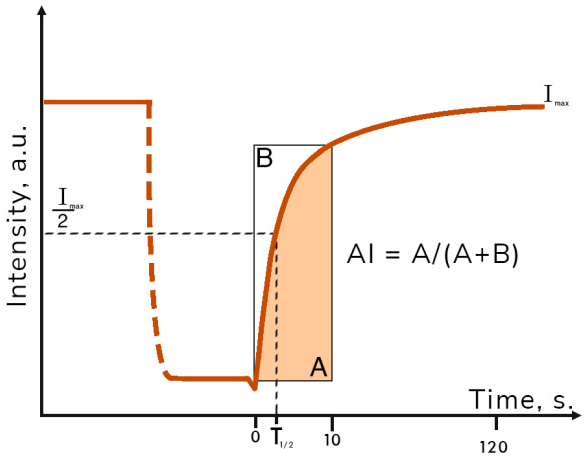

Fig. 1. The forward scattered light intensity (I) as the function of time during RBC spontaneous aggregation. The explanation of aggregation index (AI) calculation.

Additionally, the RBC spontaneous aggregation kinetic (see Fig. 1) was approximated by two exponential functions (see Eq. (1)). Time of linear (τ_1), and time of 3D aggregates (τ_2) formation were calculated:

$$I(t) = A_1 * \exp^{-\frac{t}{\tau_1}} + A_2 * \exp^{-\frac{t}{\tau_2}} + I_o, \qquad (1)$$

I is the intensity of forward scattered light; t is the time; A_1, A_2, I_o, τ_1, and τ_2 are the fitting parameters for approximation.

For RSD-K01 chip, a whole blood sample was placed into one of two reservoirs connected by a 200 μm thick channel.[23] The channel was illuminated with a laser (635 nm) and back-scattered light was detected. The initial moment of measurement is characterized by a large pressure difference between the two reservoirs of the cuvette, and therefore by large shear stresses (see Fig. 2). As the blood flows through the channel, the RBCs begin to disaggregate, i.e., the average size of the scattering particles decreases, and the particles begin to scatter more light at larger angles, resulting in an increase in backscattered light intensity. As the pressure between the reservoirs gradually decreases, at some point the RBCs begin to reaggregate, which leads to

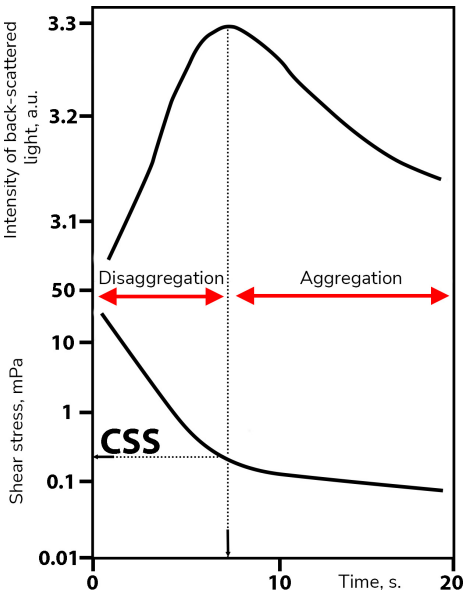

Fig. 2. The explanation of critical shear stress (CSS) calculation; (above) the intensity of backscattered light as the function of time during RBC disaggregation, and spontaneous aggregation; (below) the shear stress as the function of time.

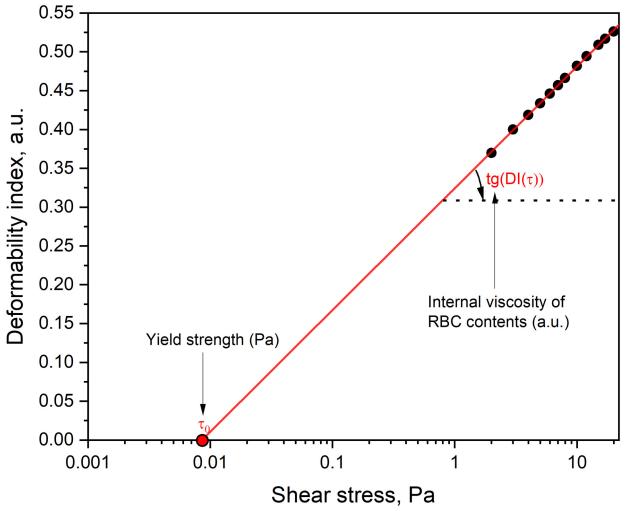

Fig. 3. Deformability index as the function of shear stress in semi logarithmic axes. The explanation of yield strength and RBC intracellular viscosity calculation.

an increase in the average particle size. Consequently, the power of light scattered backward decreases. The extreme value of the backscattered light intensity vs. time function characterizes the point in time when the aggregation, and disaggregation processes are equal (see Fig. 2). The shear stress corresponding to this extreme value is called critical shear stress (CSS). It characterizes the hydrodynamic strength of RBC aggregates.

2.2.2. *Laser ektacytometry technique*

Measurements of the RBC deformation were performed using laser ektacytometry technique.[25] It is based on the analysis of the shapes of the diffraction patterns from a highly diluted suspension of RBCs moving in a shear flow when they are illuminated by a laser beam. When the RBCs elongate due to shear stress in the flux, the diffraction pattern elongates almost in the same way in the perpendicular direction to the flow and deformation index (DI) for a certain shear stress can be calculated (Eq. (2)).[25] Thus, it is possible to obtain a quantitative characteristic of the ability of the cells ensemble to deform as a function of shear stresses[26]:

$$\mathrm{DI} = \frac{A - B}{A + B}, \tag{2}$$

where A is the long axis of the elongated diffraction pattern; B is the short axis of the elongated diffraction pattern.

Additionally, the dependence of DI on shear stress was approximated in semi-log scale by linear regression, which allowed for calculating the yield strength and the RBC intracellular viscosity (Fig. 3). In detail, the determination of RBC yield stress and RBC intracellular viscosity using deformation index measurements was described by Firsov and coauthors.[27] Briefly, the change in the RBC intracellular viscosity can be estimated by the change in slope of the dependence of the DI on the logarithm of the shear stress, and yield strength characterizing the RBC membrane rigidity can be judged from the intersection of the X-axis. The yield strength corresponds to the minimum shear stress required to initiate RBC deformation, and the RBC intracellular viscosity corresponds to the viscosity of the RBC contents (hemoglobin, etc.).

2.3. *Statistical analysis*

The parameters measured on RSA-C01 chip (AI, τ_1, and τ_2) and DI parameter were measured at least 4 times for all samples for each donor. CSS parameter was measured at least 7 times for all samples for each donor.

All data were processed, and all figures were plotted using application developed on Python. The figures below are plotted using Box plot in Tukey's

original definition. The box extends from the first quartile (Q1) to the third quartile (Q3) of the data, with a line at the median. The whiskers extend from the minimum (Q0) to the maximum value (Q4) of the data set, excluding any outliers. Outliers are values that exceed the boundaries of the box by 1.5 times the interquartile range (IQR) and are displayed by punctured points.[28]

Statistical differences between samples were calculated using Mann–Whitney U test. Two samplings were considered statistically significantly different if the p-value was less than 0.05 or 0.01 or 0.001 ($*p < 0.05$; $**p < 0.01$; $***p < 0.001$).

3. Results

As was noted in the Statistical analysis section, all figures below are plotted using Box plot. EDTA K3 samples are marked by purple colors; lithium heparin samples are marked by green colors; dextran samples are marked by blues colors.

3.1. *RBC aggregation*

The obtained results for the AI, τ_1, and τ_2 parameters at different concentrations of SNP are shown in Fig. 4. It is known that heparin is an inducer of

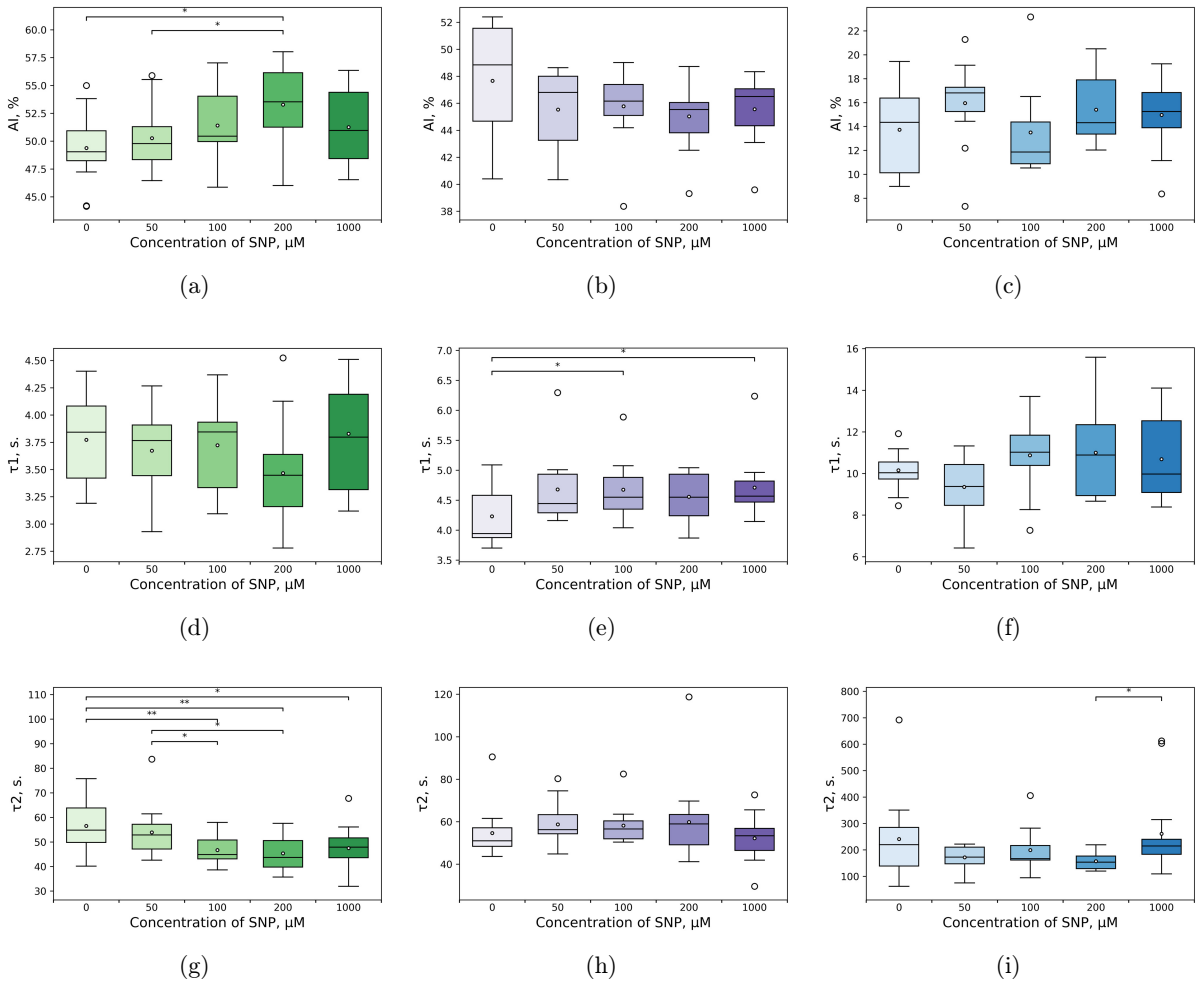

Fig. 4. (a–b) The dependence of aggregation index (AI) on the concentration of sodium nitroprusside (SNP); (a) in blood stabilized by lithium heparin, (b) in blood stabilized by EDTA K3 or (c) in washed RBC in dextran solution (130 kDa, 24 mg/mL). (d–f) The dependence of aggregation index (τ_1) on the concentration of sodium nitroprusside (SNP); (d) in blood stabilized by lithium heparin, (e) in blood stabilized by EDTA K3 or (f) in washed RBC in dextran solution (130 kDa, 24 mg/mL). (g–i) The dependence of aggregation index (τ_2) on the concentration of sodium nitroprusside (SNP); (g) in blood stabilized by lithium heparin, (h) in blood stabilized by EDTA K3 or (i) in washed RBC in dextran solution (130 kDa, 24 mg/mL). The box corresponds to the first (Q1), and to the third quartile (Q3) of the data, with a line at the median. The whiskers extend from the minimum (Q0) to the maximum value (Q4) of the data set, excluding any outliers. Mean values correspond to the white dots in the center. $*p < 0.05$; $**p < 0.01$.

RBC aggregation.[5] It explains the differences in the control values between lithium heparin end EDTA K3 samples (e.g., Figs. 4(a) and 4(b)). In heparin stabilized blood, there is an increase in RBC aggregation when adding SNP. Especially, it is well shown in the decrement of the 3D aggregates time formation (τ_2) (Fig. 4(g)).

However, in blood with EDTA anticoagulant, only the tendency to a decrease in RBC aggregation is expressed. No statistically significant differences were found for AI parameter (Fig. 4(b)), and statistically significant differences were observed for τ_1 parameter.

For the dextran solution, there is a tendency for RBC aggregation to decrease at SNP concentrations of 100 μM (Figs. 4(c) and 4(f)). No statistically significant differences were found.

3.2. *Hydrodynamic Strength of RBC aggregates*

The obtained results for the CSS parameter at different concentrations of SNP are shown in Fig. 5. Here a significant difference between different media in which RBC aggregation occurs when adding SNP is also observed. In particular, a decrease in CSS in heparinized blood was observed at SNP concentrations of 200 μM (Fig. 5(a)), whilst in dextran solution, an increase in CSS is observed at SNP concentrations above 100 μM (Fig. 5(c)).

It seems that CSS does not depend on SNP concentration for EDTA samples Fig. 5(b). CSS parameter differs from other RBC aggregation parameters as far as it defines the strength of RBC aggregates and does not characterize RBC aggregation directly.

3.3. *RBC deformation*

The obtained results for the yield strength and RBC intracellular viscosity parameters at different concentrations of SNP are shown in Fig. 6. There is some correspondence between heparin, and dextran samples as far as there is a decrease in yield strength and an increase in RBC intracellular viscosity at SNP concentrations of 100 μM (Figs. 6(a) and 6(c)).

4. Discussion

4.1. *RBC aggregation*

The obtained data considerably differ from those obtained when studying RBC aggregation in dextran solution using the flow chamber,[9] i.e., there was a significant decrease in RBC aggregation at 100 μM concentration of SNP, whereas in this work, a tendency for a decrease in aggregation at 100 μM concentration of SNP was observed for dextran solution and even an increase in RBC aggregation was observed in heparinized blood. The reason for these differences may lie in different methods, blood preparation, and RBC samples (for example, different hematocrit conditions — in work[9] it was about 1%, while in our work it was in the range of whole blood values (40–45%)). This means that nitric oxide can be both an inducer and an inhibitor of RBC aggregation, depending on the environment, in which the cells aggregate. Since the main

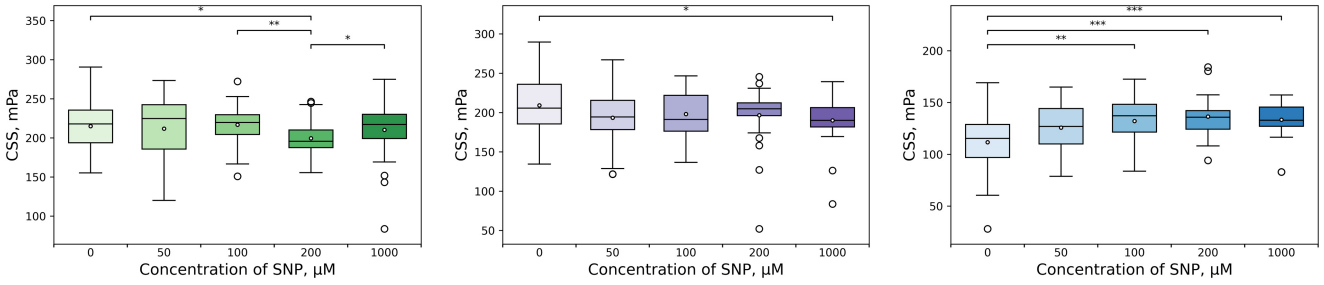

Fig. 5. (a–b) The dependence of critical shear stress (CSS) on the concentration of sodium nitroprusside (SNP); (a) in blood stabilized by lithium heparin, (b) in blood stabilized by EDTA K3 or (c) in washed RBC in dextran solution (130 kDa, 24 mg/mL). The box corresponds to the first (Q1), and to the third quartile (Q3) of the data, with a line at the median. The whiskers extend from the minimum (Q0) to the maximum value (Q4) of the data set, excluding any outliers. Mean values correspond to the white dots in the center. *$p < 0.05$; **$p < 0.01$; ***$p < 0.001$.

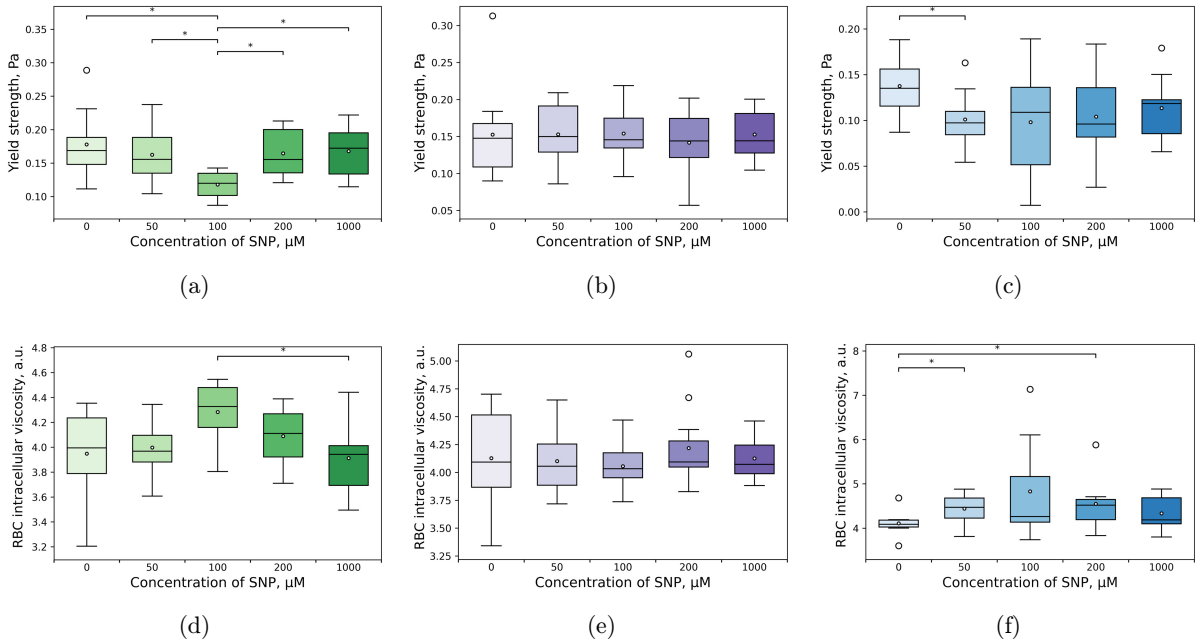

Fig. 6. (a–b) The dependence of yield strength of RBC on the concentration of sodium nitroprusside (SNP); (a) in blood stabilized by lithium heparin, (b) in blood stabilized by EDTA K3 or (c) in washed RBC in dextran solution (130 kDa, 24 mg/mL). (d–f) The dependence of RBC intracellular viscosity on the concentration of sodium nitroprusside (SNP); (d) in blood stabilized by lithium heparin, (e) in blood stabilized by EDTA K3 or (f) in washed RBC in dextran solution (130 kDa, 24 mg/mL). The box corresponds to the first (Q1), and to the third quartile (Q3) of the data, with a line at the median. The whiskers extend from the minimum (Q0) to the maximum value (Q4) of the data set, excluding any outliers. Mean values correspond to the white dots in the center. $*p < 0.05$.

difference in the action between the two anticoagulants (EDTA K3, and lithium heparin) is the preservation or almost complete binding of calcium in the blood, it seems that calcium acts as a regulator in the mechanisms of action of nitric oxide on RBC aggregation properties.

4.2. *Hydrodynamic strength of RBC aggregates*

Dextran molecules have been shown to adsorb on the RBC membrane, which directly affects RBC aggregation.[29] The increase in CSS for dextran solution may be due to the change in the adsorption of dextran molecules at different SNP concentrations. Further studies are required.

4.3. *RBC deformation*

The measured characteristics of RBC deformability, such as yield stress, and RBC intracellular viscosity, were not found to be sensitive to SNP concentration in the range up to 1 mM in EDTA-stabilized blood samples (Fig. 6(b)). It may be caused by the absence of calcium ions in this blood sample. However, there is evidence to suggest that the deformability of RBCs from EDTA-stabilized blood increases with the addition of SNP, as observed in measurements made for washed RBCs.[30]

Bivalent calcium ions play a major role in the maintenance of RBC mechanical state. It is known that an increase in intracellular Ca^{2+}+ concentration leads to impairment in RBC deformability.[31] Some results suggest that SNP interacts with thiol groups of RBC membrane proteins and forms nonspecific disulfide bonds, which inhibit calcium influx.[32] Thus, SNP prevents intracellular Ca^{2+} accumulation and has a protective effect. This also means that the protective effect of SNP on RBC deformation might only occur in media in which Ca^{2+} is present. In this case, it is consistent with the results showing that SNP significantly decreased the yield stress of RBC in heparinized blood (Fig. 6(a)) and did not have a significant effect in the EDTA blood sample (Fig. 6(a)). Additionally, since RBC undergo external mechanical stress during ektacytometry measurements, the mechanosensitive Piezo1 receptor complex localized on the membrane can be activated. This leads to the intensification of

Ca^{2+} channels, which regulate the activity of protein kinase C, Calcium-ATPase, and Gardos channels that affect RBC deformability properties.[33] Therefore, significant alterations in RBC deformability can be expected upon the addition of SNP through metabolic pathways in Ca^{2+}-supplemented media.

5. Conclusion

The results demonstrate a complex behavior of RBC aggregation, and deformation parameters measured *in vitro* with sodium nitroprusside depending on the sample preparation, and medium, in which RBC can aggregate or deform. It seems that the medium itself may be an additional factor in altering the action of sodium nitroprusside, which should be considered when determining the role of sodium nitroprusside in RBC aggregation. This suggests that the effect of nitric oxide donor sodium nitroprusside on RBC aggregation is directly related to the media in which RBC aggregation occurs. In future studies, it is important to take this into account because different media and different anticoagulants are used in different studies of RBC aggregation, and deformation properties.

Acknowledgments

All experiments conducted by laser aggregometry, and ektacytometry, as well as the purchase of consumables, blood drawing, and blood delivery, the development of protocols, receiving the ethics committee permission were supported by the Russian Science Foundation grant (No. 22-15-00120). The data analysis conducted by Petr Ermolinskiy was supported by the grant (No. 21-2-10-59-1) from the Foundation for the Development of Theoretical Physics and Mathematics BASIS.

Conflicts of Interest

The authors declare that they have no conflict of interest.

References

1. M. Diez-Silva, M. Dao, J. Han, C. Lim, S. Suresh, "Shape and biomechanical characteristics of human red blood cells in health and disease," *MRS Bulletin* **35**, 382–388 (2010).
2. C. Geers, G. Gros, "Carbon dioxide transport and carbonic anhydrase in blood and muscle," *Physiol. Rev.* **80**, 681–715 (2000).
3. A. Gillespie, A. Doctor, "Red blood cell contribution to hemostasis," *Front. Pediatr.* **9**, 1–9 (2021).
4. L. Anderson, I. Brodsky, N. Mangalmurti, "The evolving erythrocyte: Red blood cells as modulators of innate immunity," *J. Immunol.* **201**, 1343–1351 (2018).
5. O. Baskurt, B. Neu, H. Meiselman, *Red Blood Cell Aggregation*, CRC Press, Boca Raton, USA (2012).
6. M. W. Rampling, H. J. Meiselman, B. Neub, O. K. Baskurt, "Influence of cell-specific factors on red blood cell aggregation," *Biorheology* **41**, 91–112 (2004).
7. K. Lee, A. Danilina, A. Potkin, M. Kinnunen, A. Priezzhev, I. Meglinski, "RBC aggregation dynamics in autologous plasma and serum studied with double-channel optical tweezers," *Proc. SPIE*, **9917**, 991704 (2016).
8. A. Muravyov, I. Tikhomirova, "Role of molecular signaling pathways in changes of red blood cell deformability," *Clin. Hemorheol. Microcirc.* **53**, 45–59 (2012).
9. A. Muravyov, "The role of gaseous mediators (CO, NO and H_2S) in the regulation of blood circulation: Analysis of the participation of blood cell microrheology [in Russian]," *Reg. Blood Circ. Microcirc.* **20**, 91–99 (2021).
10. N. Tran, T. Garcia, M. Aniqa, S. Ali, A. Ally, S. Nauli, "Endothelial nitric oxide synthase (enos) and the cardiovascular system: In physiology and in disease states," *Am. J. Biomed. Sci. Res.* **15**, 153–177 (2022).
11. L. Ignarro, C. Napoli, J. Loscalzo, "Nitric oxide donors and cardiovascular agents modulating the bioactivity of nitric oxide — an overview," *Circ. Res.* **90**, 21–8 (2002).
12. M. Cortese-Krott, M. Kelm, "Endothelial nitric oxide synthase in red blood cells: Key to a new erythrocrine function?" *Redox Biol.* **2**, 251–258 (2013).
13. A. Muravyov, P. Avdonin, I. Tikhomirova, S. Bulaeva, J. Malysheva, "Effects of gasotransmitters on membrane elasticity and microrheology of erythrocytes," *Biochem. Moscow Suppl. Ser. A* **13**, 225–232 (2019).
14. M. Bor-Kucukatay, R. Wenby, H. Meiselman, O. Baskurt, "Effects of nitric oxide on red blood cell deformability," *Am. J. Physiol. Heart Circ. Physiol.* **284**, H1577–H1584 (2003).
15. P. Ulker, N. Yaras, C. Celik-Ozenci, H. Meiselman, O. Baskurt, "Shear stress activation of nitric oxide synthase and increased no levels in human red blood cells," *Nat. Preced.* **5**, 1–13 (2010).

16. A. Mozar, P. Connes, B. Collins, H.-D. MD, M. Romana, N. Lemonne, W. Bloch, M. Grau, "Red blood cell nitric oxide synthase modulates red blood cell deformability in sickle cell anemia," *Clin. Hemorheol. Microcirc.* **64**, 728–736 (2015).
17. A. Pribush, D. Zilberman-Kravits, N. Meyerstein, "The mechanism of the dextran-induced red blood cell aggregation," *Eur. Biophys. J.* **36**, 85–94 (2007).
18. A. N. Semenov, A. Lugovtsov, P. Ermolinskiy, K. Lee, A. V. Priezzhev, "Problems of red blood cell aggregation and deformation assessed by laser tweezers, diffuse light scattering and laser diffractometry," *Photonics* **9**(4), 1–19 (2022).
19. M. Uyuklu, M. Cengiz, P. Ulker, T. Hever, J. Tripette, P. Connes, N. Nemeth, H. Meiselman, O. Baskurt, "Effects of storage duration and temperature of human blood on red cell deformability and aggregation," *Clin. Hemorheol. Microcirc.* **41**, 269–278 (2009).
20. A. V. Priezzhev, K. Lee, N. N. Firsov, J. Lademann, "Optical study of RBC aggregation in whole blood samples and single cells," *Handbook of Optical Biomedical Diagnostics*, V. V. Tuchin, Ed., Vol. 2, pp. 5–36, 2nd Edition, SPIE PRESS, Bellingham, USA (2016).
21. S. Shin, Y. Yang, J. Suh, "Measurement of erythrocyte aggregation in a microchip stirring system by light transmission," *Clin. Hemorheol. Microcirc.* **41**, 197–207 (2009).
22. J. Kim, H. Chung, M. Jo, B. Lee, A. Karimi, S. Shin, "The role of critical shear stress on acute coronary syndrome," *Clin. Hemorheol. Microcirc.* **55**, 101–109 (2013).
23. P. B. Ermolinskiy, A. N. Semenov, A. E. Lugovtsov, C. Poeschl, U. Windberger, E. Kaliviotis, A. V. Priezzhev, "Effect of different macromolecules on viscous and microrheologic properties of blood at various temperatures," *Proc. SPIE*, **11065**, 1106507-1–1106507-5 (2019).
24. J. Mauer, M. Peltomäki, S. Poblete, G. Gompper, D. Fedosov, "Static and dynamic light scattering by red blood cells: A numerical study," *PLoS ONE* **12**, 1–19 (2017).
25. O. Baskurt, M. Hardeman, M. Uyuklu, P. Ulker, M. Cengiz, N. Nemeth, S. Shin, T. Alexy, H. Meiselman, "Comparison of three commercially available ektacytometers with different shearing geometries," *Biorheology* **46**, 251–264 (2009).
26. J. Gounley, Y. Peng, "Computational modeling of membrane viscosity of red blood cells," *Commun. Comput. Phys.* **17**, 1073–1087 (2015).
27. N. N. Firsov, A. V. Priezzhev, N. V. Klimova, A. Y. Tyurina, "Fundamental laws of the deformational behavior of erythrocytes in shear flow," *J. Eng. Phys. Thermophys.* **79**(1), 118–124 (2006).
28. J. Grice, "Graphical exploratory data analysis," *Technometrics* **31**, 116–117 (2012).
29. K. Lee, E. Shirshin, N. Rovnyagina, F. Yaya, Z. Boujja, A. Priezzhev, C. Wagner, "Dextran adsorption onto red blood cells revisited: Single cell quantification by laser tweezers combined with microfluidics," *Biomed. Opt. Express* **9**(6), 2755–2764 (2018).
30. E. Nader, M. Romana, N. Guillot, R. Fort, E. Stauffer, N. Lemonne, Y. Garnier, S. C. Skinner, M. Etienne-Julan, M. Robert, A. Gauthier, G. Cannas, S. Antoine-Jonville, B. Tressières, M.-D. Hardy-Dessources, Y. Bertrand, C. Martin, C. Renoux, P. Joly, M. Grau, P. Connes, "Association between nitric oxide, oxidative stress, eryptosis, red blood cell microparticles, and vascular function in sickle cell anemia," *Front. Immunol.* **11**, 1–13 (2020).
31. L. Kuck, J. N. Peart, M. J. Simmonds, "Calcium dynamically alters erythrocyte mechanical response to shear," *Biochim. Biophys. Acta Mol. Cell Res.* **1867**(11), 118802 (2020).
32. V. Barodka, J. G. Mohanty, A. K. Mustafa, L. Santhanam, A. Nyhan, A. K. Bhunia, G. Sikka, D. Nyhan, D. E. Berkowitz, J. M. Rifkind, "Nitroprusside inhibits calcium-induced impairment of red blood cell deformability," *Transfusion* **54**(2), 434–444 (2013).
33. N. Cilek, E. Ugurel, E. Goksel, O. Yalcin, "Signaling mechanisms in red blood cells: A view through the protein phosphorylation and deformability," *J. Cell. Physiol.* (2023).